8-16-2024

Cell Based Sodium Alginate Microcapsules Within Ocular Disease: A Proof of Concept

Chelsea Marie Zizzi
University of South Carolina

CELL BASED SODIUM ALGINATE MICROCAPSULES WITHIN OCULAR DISEASE: A PROOF OF CONCEPT

by

Chelsea Marie Zizzi

Bachelor of Science
Ferrum College, 2022

Submitted in Partial Fulfillment of the Requirements

For the Degree of Masters of Science in

Biomedical Sciences

School of Medicine

University of South Carolina

2024

Accepted by:

Jay Potts, Director of Thesis

Robert Price, Reader

Colin Evans, Reader

Ann Vail, Dean of the Graduate School

DEDICATION

To my Dad, Mother, and Sister. Their support and understanding has allowed me to soar into possibilities that I never fathomed I could reach. Thank you all for giving me the strength to try new things, because you never know, “you might be changed turtle”.

ACKNOWLEDGMENTS

I would like to thank the University of South Carolina School of Medicine and the faculty and staff that have helped me along the way. I would like to profusely thank my major professor, Dr. Jay D. Potts. Your 'tough love' demeanor has pushed me to be a better scientist and constantly challenge myself; thank you for setting me up to be the best researcher I can be. Thanks to my committee members, Dr. Robert Price and Dr. Colin Evans, alongside with Dr. Austin Worden, who has helped me become a better scientific writer. Another acknowledgment I would like to bring to light would be to Quinn Fowler, who has helped me at the start of lab through means of staining and imaging. Further, I would like to thank Kasie Roark and Raymond Bogdon, who offered support when it was most needed. I also wanted to thank the Instrumentation Resource Facility and the biotech 'crew' including Anna Harper and Lorain Junor, and all the students within the biotech concentration. This research could not have happened without funding from the National Institute of General Medical Sciences of the National Institutes of Health under Award Number P20GM103499 as well as the Jack and Miriam Webb Vision Research Fund. You all have been an imperative part of this process. Thank you.

ABSTRACT

Sodium alginate is a natural polymer that has been widely used as a drug delivery system due to its controlled-release qualities and low cellular toxicity. These capsules are effective at transporting therapeutics in various diseased animal models. Retinitis Pigmentosa is an incurable genetic disease affecting the retina, which causes gradual blindness as the disease progresses. In our study, we injected cell-based sodium alginate capsules into the vitreous cavity of C57BL/6 and *Pde6b*^{rd10}/J mice to observe the migration of these capsules in both wildtype and diseased mouse models over a course of 2 weeks. Our intention was to utilize the slow-release factor of sodium alginate and to prove the possibility of retinal regeneration using arising retinal pigmented epithelial cells or adipose stem cells. We observed that there seems to be a proximal effect from these cell-based microcapsules on the ganglion cell layer as well as these cells affecting the lens. While our work is in the preliminary stages, this project shows that cell-based sodium alginate microcapsules are a viable source to treat ocular diseases.

TABLE OF CONTENTS

LIST OF FIGURES

LIST OF ABBREVIATIONS

ADSC.....Adipose-Derived Stem Cells

Ampho B.....Amphotericin B

ARPE ..... Arising Retinal Pigmented Epithelial Cells

DMEM.....Dulbecco's Modified Eagle Medium

FBS.....Fetal Bovine Serum

H&E .....Hematoxylin and Eosin

HEPES .....2-(4-(2-hydroxyethyl)piperazin-1-yl)ethane sulfonic Acid

MC .....Müller Cells

mDF .....Modified Davidson's Fixative

PFA .....Paraformaldehyde

PS .....Penicillin-Streptomycin

RPE ..... Retinal Pigmented Epithelium

TBS .....Tris-Hydrochloric Acid Buffered Saline Solution

CHAPTER 1

INTRODUCTION

Anatomy of the Eye

The eye is a complex sensory organ that consists of physical barriers, microenvironment, and regulatory systems that make it immune privileged [1]. To fully understand the complexity of the eye and how vision works, one must understand the parts within the eye. The internal structure of the eye is composed of three layers including the exterior, vascular tunic, and innermost layers [2, 3]. The exterior layer, also known as the fibrous tunic, contains both the sclera and cornea. The sclera is the white portion of the eye that is responsible for protection and giving the eye its general shape, while the cornea covers the iris and plays a pivotal role in oxygen homeostasis [4]. Both the sclera and cornea are composed of type 1 collagen fibers; however, the orientation of these fibers, parallel fibers within the sclera and perpendicular within the cornea, gives the sclera its white color and leaves the cornea transparent [2, 3]. The border between the sclera and cornea is the limbus, a common site for surgical injections [5]. The exterior layer is the first line of defense to protect the inner sections of the eye.

Beneath the external layer is the vascular tunic, which is also known as the uvea [2, 3]. This layer consists of the choroid, the iris, and the ciliary body. Lining the sclera is the choroid, which contains blood vessels critical for nutrient exchange between structures within the eye. The iris is the colored portion of the eye and is located between

the lens and cornea. The iris is composed of melanin and is able to regulate the amount of light that reaches the pupil by either contracting or expanding. In addition, the choroid also produces melanin which further restricts scattered light from reaching the retina. The ciliary body contains two parts: the ciliary epithelium and the ciliary muscle. The main function of the ciliary epithelium is the production of aqueous humor, which is the fluid that fills the space between the lens and the cornea. The ciliary muscle controls the zonular fiber tightness which alters the shape of the lens for distal and proximal vision [2, 3]. The middle sections of the eye eliminate sporadic photons and provide means of transportation of nutrients and molecules to further progress phototransduction with the inner layers of the eye.

The final layer of the eye consists of the lens, vitreous, and retina. The lens is created peripherally; newer lens cells will push older cells toward the center of the lens where they will elongate and create secondary fibers [6]. The lens is located behind the pupil and iris and divides the eye into two sections: the anterior and vitreous cavities. The anterior cavity is found between the cornea and iris as well as behind the iris. This cavity is filled with aqueous humor, which is regularly replaced to maintain intraocular pressure, homeostasis, and a transparent microenvironment for effective light transmission [7]. The vitreous cavity lies between the lens and the retina. It is full of vitreous humor, a gel-like substance that contains phagocytes responsible for the elimination of unwanted substances that could affect phototransduction within the retina [2, 3].

The Retina

The retina is a complex extension of the central nervous system. There is a multitude of layers to the retina that work cooperatively to relay information to the brain including the retinal pigmented epithelium (RPE), photoreceptor layer, outer nuclear layer, outer plexiform layer, inner nuclear layer, inner plexiform layer, and ganglion cell layer respectively [8]. These layers can be seen in Figure 1.1. When light enters the retina, the RPE will absorb and reduce the light that is reflected to the photoreceptor cells. This causes a cascade of events leading to information being carried through the optic nerve to the brain and processed in the visual cortex [8].

The outer side of the RPE forms a blood-retina barrier, maintaining homeostatic stability of the microenvironment within the retina while the inner side of the RPE is connected to the photoreceptor cell layer through apical microvilli structures that extend between the outer segment of the photoreceptor cells [9]. These structures participates in the phagocytic function of the RPE [10]. Aged regions of the outer segment of the photoreceptor layer undergo damage from photo-oxidation and must be removed through phagocytosis before damaging neighboring photoreceptor cells [10]. Inflammation stress is also a cause of RPE and photoreceptor degeneration; extracellular debris beneath the RPE elicit inflammation and an immune response that, if not removed, will cause degeneration [11]. The phagocytosis by the RPE is the only clearance means for these photoreceptor segments, and without it, the photoreceptor layer will deplete and cause retinal disorders [10]. To mitigate some photoreceptor damage, the RPE contains melanin to reduce toxicity by acting as a free radical sink for stray photons, thus reducing photo-oxidation [12].

The photoreceptor layer converts photons into neuronal responses through the rods and cones. Rods are highly sensitive to light, outnumber cones 20:1 [13], and provide adequate vision in low-light environments. Cones, in comparison, are less sensitive than rods but have a faster kinetic response during phototransduction [14]. While rods are concentrated within the periphery, cones are centralized in the retina. Nocturnal animals, like the laboratory mouse, have rod-dominate retinas whereas diurnal animals have cone-rich retinas [13]. It is to be noted that dinural animals still possess more rods than cones; however, they have more classes of cones within the retina.

There are four different classes of cone photoreceptors including S cones, M cones, L cones, and UV cones meaning short, medium, long, and ultraviolet wavelength respectively. Cone types differ across species; most mammals have S and M cones, whereas humans have L cones, and fish and birds have UV cones. The ratio of cone classes also differs across species; for example, S cones in a monkey retina are distributed in a precise manner whereas they are randomized in a human retina even though both species share the same types of cones [9] [15].

Bipolar cells provide an intraretinal connection between photoreceptor cells and ganglion cells [16]. The majority of intraretinal feedback to bipolar cells are mediated by amacrine cells [17]. Amacrine cells are interneurons representing the most diverse class of neurons in the retina. Mammalian amacrine cells can further be defined by their subtypes. Diffuse cells extend throughout the inner plexiform layer, whereas stratified cells do not [18]. Amacrine cells form gap junctions with other amacrine cells, which transport light signals to cones to turn them on or off [19].

The nuclei of rods, cones, and bipolar cells are found in the outer nuclear layer. Since rods outnumber cones, they account for most of the outer nuclear layer except at the fovea. The fovea is a small dip within the retina where visual acuity is the highest [20]. Preceding the outer nuclear layer is the outer plexiform layer. This layer includes synapses between axons of photoreceptor cells and dendrites of intermediate neurons, which connect it to the inner nuclear layer. Inside the inner nuclear layer of the retina lie the cell bodies of intermediate neurons, amacrine cells, horizontal cells, and Müller cells (MCs). Neurons interact laterally with the outer plexiform layer axons to induce light sensitivity within the retina [21].

Horizontal cells are viewed as the primary cells for receiving information from rods and cones [22]. These cells project laterally within the retina and mainly show a connection with cone photoreceptors [23]. Rod photoreceptor cell signals are connected to horizontal cells through cone axon terminals [22]. The terminals in these two cell types consist of single (rods) and multiple (cones) ribbons that mediate active zones where second-order neurons receive signals to group exocytosis-related vesicles [24]. Photoreceptor cell signals are coupled at their axon terminals, but studies have shown that signals from rods do not travel along horizontal axons to its axon terminus whereas cone signals do [24].

Of the three glial cell types in the retina, MCs are the most common and most closely related to retinal neurons [25]. MCs support photoreceptor and neuronal transmission into the vasculature, allowing for regulated product exchange of ions and water [26]. These cells are one of the last to develop within the retina and maintain homeostasis through the modulation of ion transportation to maintain the composition of

extracellular space fluid [25] [27]. Additionally, they guide light through the inner nuclear layer and provide anti-oxidative support for a non-toxic environment [27].

Following the inner nuclear layer are the inner plexiform layer and the ganglion cell layer. The inner plexiform layer is the synapse between intermediate neurons and ganglion cells of the optic tract [8]. Ganglion cell axons coalesce at the optic disc forming the optic nerve, which then transmits visual information to the visual cortex [8]. Due to the many retinal components and complexities, there are abundant chances for system disruption that can produce a toxic environment. These toxic environments are considered ocular diseases.

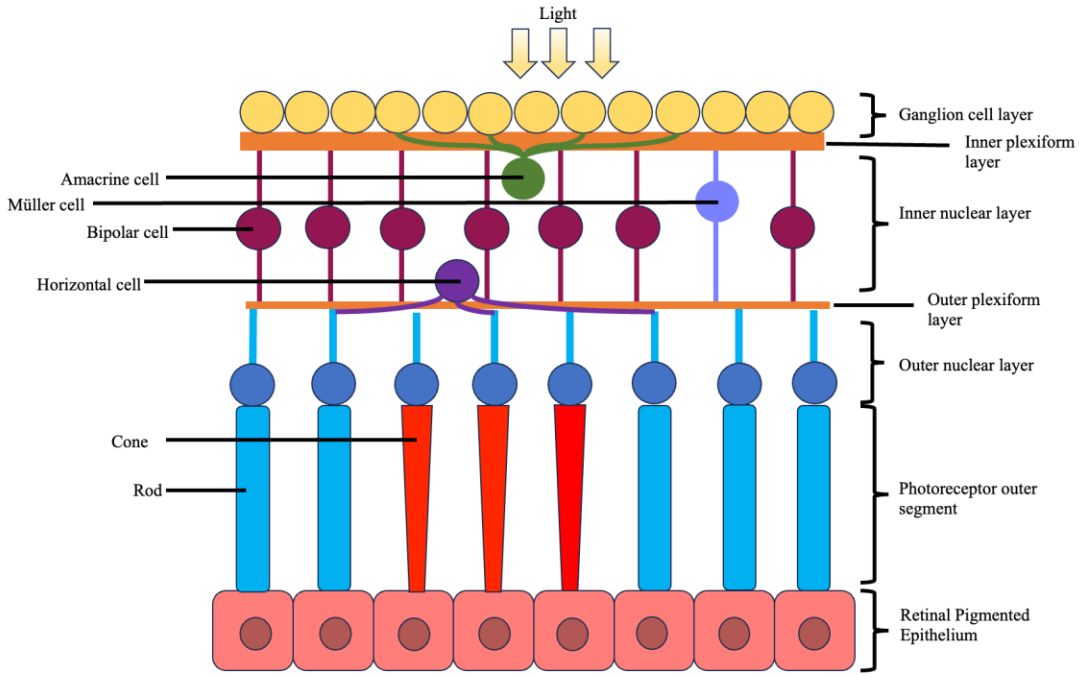

Figure 1.1: Diagram of cells within the retina

Ocular Disease

Ocular disease is a term representing the diseases that affect the eye's health or function, leading to less movement or blindness. Since the eye is part of the central nervous system, it is seen as an extension of the brain [28]. As such, these ocular diseases can also correspond with brain-related degeneration such as macular degeneration, glaucoma, and amblyopia or 'lazy eye'. Similarly, retinal imaging has been used as an early detection and tracker for Alzheimer's disease as well as other neurological degenerative diseases [28, 29].

Two of the leading causes of blindness worldwide are macular degeneration and glaucoma [30]. Inflammation is a cofactor in pathogenesis of such diseases [31]. Inflammation can be caused by environmental factors and irregular metabolism within the eye; drusen, which is an accumulation of extracellular matrix between the RPE and choroid, will cause morphological and pigmentation changes leading to localized inflammation that degrades the RPE. The RPE regulates pro- and anti- inflammatory cytokines and degradation of the RPE will lead to chronic inflammation [31].

Another factor that causes ocular diseases is oxidative stress [32]. Oxidative stress is caused by an increase in reactive oxidizing agents through means of an unbalanced redox homeostasis. This unbalance can cause changes in mitochondrial function throughout the eye. Mitochondria are believed to mutate at a quicker rate than cell DNA in high oxidative environments through the electron transport chain oxidative phosphorylation process; however, high oxidative environments can lead to DNA and

protein modifications that will disrupt cellular function [32]. One example of an ocular disease that can occur from oxidative stress is Retinitis Pigmentosa.

Retinitis Pigmentosa

Retinitis Pigmentosa is an untreatable genetic disease that causes photoreceptor cell death and RPE degeneration through means of oxidative stress and inflammation. The name Retinitis Pigmentosa is a misnomer that is often mistaken for color blindness rather than total blindness. The first symptoms of Retinitis Pigmentosa is night blindness and peripheral vision loss, eventually leading to tunnel vision or total blindness depending on disease progression. Retinitis Pigmentosa typically affects both eyes, but there are some cases where only one eye has retinal degeneration [33]. Retinitis Pigmentosa affects 1 out of 4000 people in the United States, and around 1 out of 5000 worldwide [33]. Most patients present symptoms leading to Retinitis Pigmentosa diagnosis around 30 years or age; furthermore, the majority of Retinitis Pigmentosa cases are nonsyndromic with around 30% being syndromic [33]. Although there is no current treatment for Retinitis Pigmentosa, most studies show that the best results yield from therapeutics before any photoreceptor cell death. The most common remedy is supplementation with vitamin A, which is said to slow the progression of retinal degradation [33]. The first two layers of the retina, the RPE and photoreceptor cells, are the layers primarily affected by Retinitis Pigmentosa.

One of the major factors of Retinitis Pigmentosa is retinal toxicity through photoreceptor degradation and free radical production. Oxygen consumption within the retina is related to the number of rods; therefore, as rods degrade, oxygen concentration

within the retina increases, thus increasing the probability of free radicals within the retina and toxic environments [34]. These highly reactive radicals impact body systems including the electron transport chain and NADPH oxidase eventually producing more oxyanions that result in photoreceptor cell death [34]. In this environment, degradation of rods occurs eventually leading to autophagy of cones and the RPE [34]. However, mutations can occur that cause cone death and do not affect rod cells [35].

Retinitis Pigmentosa is associated with different mutations in over 80 genes and can arise from certain diseases such as Usher syndrome type 2, which is the most recurrent form of recessive syndromic Retinitis Pigmentosa [36, 37]. Most genes that are affected are rod-specific genes, whereas other genes, like RPE65, tend to deal with the RPE and other retinal cells [38]. One gene of interest is phosphodiesterase 6B, or Pde6b gene. Pde6b is part of the cGMP-PDE protein complex, which is found in rod cells [39]. This disease is inherited as autosomal dominant, autosomal recessive, or is X-linked. X-linked Retinitis Pigmentosa shows that men are more likely to develop RP as it is expressed only in males, but no significant factors show RP as a sex-limited disease [40]. However, RP progression differs between sexes [33, 41]. One study found that in the autosomal recessive rd10 mouse model, female mice show an earlier onset of disease by Pde6b protein loss compared to male mice [41]. Our lab focuses on this early-onset protein loss in *Pde6b*^{rd10}/J mouse models.

Rhodopsin and Calretinin

Rhodopsin and calretinin are proteins naturally found within the retina. Rhodopsin is a G-protein coupled receptor and is the most abundant protein found within

rod photoreceptors [42, 43]. Photoreceptor longevity is directly tied to the appropriate activation and deactivation of this protein to prevent a hypertoxic environment [42]. When activated, rhodopsin causes phototransduction and an electrical signal gradient will begin [44].

Calretinin is a calcium-binding protein that utilizes calcium buffering to modulate neuronal activity [45]. Calretinin is found in most nuclei layers of the retina but is most abundant in the ganglion cell layer [45] . Calretinin is rarely found in the photoreceptor cell layer; however, it represents the neuronal structures within the retina that are part of the signaling pathway of the brain that leads to the visual cortex based on photon gradient receptivity. Rhodopsin and calretinin are important protein markers for imaging because they represent the electrical signal gradient, starting from the photoreceptor cells to the ganglion cell layer.

Microencapsulation

Cell-based therapies are rapidly evolving techniques within the medicinal world. The primary focus of these drug delivery systems is to engineer approaches for a controlled release of therapeutic agents to target specific areas within the body [46]. These systems can be designed by understanding the biomaterials used to create these therapeutics and discovering novel biomaterials that make developing new and systematic pharmaceutical systems possible [47].

Microcapsules, as the name suggests, are spherical capsules that range around 1-1000 micrometers in diameter [48]. Microcapsules can be manipulated through changes of pH and secondary coatings to better individualize treatments. The size and shape of

microcapsules can also be changed depending on the microencapsulation technique [49]. Microcapsules are created using electrohydrodynamic techniques including vibrational jet flow, solvent evaporation, emulsion, and electrospray methods [50]. Microcapsules are advantageous because they provide a controlled release rate and protection against immune cells for active agents [51].

The electrospray technique is a widely used technique for microencapsulation [52]. For this technique to work, an anionic polymer is sprayed through a syringe pump at a specific voltage into a cationic gelling solution, which crosslinks the polymer to create hollow spheres for drug delivery applications. It is to be noted that the crosslink between the anionic polymer and cations of the gelling solution can be carried out without the use of separate equipment, temperature change, or organic solvent use [53].

Alginate

While several types of polymers can be used for encapsulation, like polymeric micelles and hyaluronic acid, our lab focuses on alginate. Alginate is an anionic polysaccharide that is found on the walls of brown algae [51]. Alginates are abundant, cost-efficient, and are used for a multitude of applications: drug delivery, wound healing, and tissue recovery [54]. Alginic acid is used to create a viscous solution that acts as the polymeric membrane for encapsulation processes [51]. Particle size, viscosity, and chemical composition of alginates influence drug release properties [55]. As the concentration of alginate increases it becomes more difficult to create microcapsules due to decreased permeability. Likewise, too low of a concentration can produce microcapsules with high permeability which are not suitable for slow release [56]. This

represents the importance of properly manufacturing alginate to yield the best therapeutic results. In addition, impurities such as heavy metals should be removed before polymer encapsulation so that it can be viable for biomedical practices [47].

Adipose-Derived Stem Cells

Microencapsulation can be used as a drug delivery system for cell-based therapies, such as adipose-derived stem cells (ADSCs). ADSCs are mesenchymal stromal cells that migrate towards wound sites and start the cell regeneration process [57]. ADSCs can differentiate into a multitude of cells including neurons and endothelial cells as well as release neurotrophic factors that deal with nerve regeneration [58, 59]. Studies have shown that ADSCs have the ability to modulate inflammation by reducing pro-inflammatory cytokines within the central nervous system [58]. ADSCs have a high potential for stem cell therapies as well as an approach for encapsulation methods.

Arising Retinal Pigmented Epithelial Cells

Another common cell studied for cell-based microencapsulation techniques are arising retinal pigmented epithelial cells (ARPE). ARPE cells can closely resemble native RPE cells if properly handled [60]. Early studies have shown that ARPE cells have a rapid proliferation rate and maintain this rate through their long life span [61]. These cells are used in long-term therapies because of their long-term survival post encapsulation and injection [62]. ARPE cells have a high proliferation rate and contain pigmentation that is comparable to in vivo RPE cells [63].

Our research utilizes the electrospray technique for microencapsulation production of cell-based ARPE and ADSC capsules. These capsules are used for

intravitreal injections to study results that can be used for ocular research in the future. Our goal is to prove the viability and specificity of alginate-based cell delivery systems and describe the effects these therapies have on the eye in hopes of treating ocular diseases like RP.

CHAPTER 2

METHODS AND MATERIALS

Mice

Male knockout *Pde6b*^{rd10}/J and wild type (C57BL/6J) mice were purchased from Jackson Laboratories (strain number 004297,000664; Bar Harbor, ME). Mice were maintained and housed under standardized conditions in accordance with the Department of Laboratory Animal Resources at the University of South Carolina School of Medicine. Animal work was conducted following the protocol approved by the Institutional Animal Care and Use Committee of the University of South Carolina. Mice that were used for experimentation were purchased at 4 weeks and experimented on between 5 and 7 weeks of age.

Cell Staining

ADSC and ARPE cell lines were cultured in Dulbecco's Modified Eagle Medium (DMEM) with 10% fetal bovine serum (FBS), penicillin-streptomycin (PS), and Amphotericin B (Ampho B). 75% confluent cell flasks were trypsinized using 0.25% trypsin ethylenediaminetetraacetic acid (EDTA), centrifuged at 800 rpm for 8 minutes, and resuspended in 4 mL of media. 2 mL of suspension with 5 mL of cell culture media were added to a 25 cm^2 flask and placed in an incubator overnight to allow cell confluency before staining. The next day the cell stain was prepped; 7.5 uL of Cell Tracker Green CMFDA was added to 3 mL of cell culture media. Cellular media was

replaced with the cell stain solution and incubated for 1 hour at 37°C. After incubation, the cell stain solution was removed and the cell encapsulation protocol was started.

Encapsulation / Cell Encapsulation

3 mL of 0.25% trypsin EDTA was added to ARPE and ADSC stained cell flasks and incubated at 37°C for 2 minutes or until the cells were floating. After the cells were floating, 6 mL of non-phenol red cell culture media was added, and all cells were transferred to separate 15 mL conical tubes and spun down at 800 RMP for 8 minutes. The media was aspirated and 300 uL of 2-(4-(2-hydroxyethyl)piperazin-1-yl)ethanesulfonic acid (HEPES) buffered saline solution was used to resuspend the cells. 1 mL of alginate was added into a 1.5 mL centrifuge tube along with 105 uL of cell/HEPES mixture. This mixture was pipetted vigorously until the cell mixture was incorporated into the alginate. Then 300 uL of this solution was added into a 3 mL syringe and a 1-inch blunt needle tip was placed on the syringe. 40 mL of warmed cell capsule gelling solution, which is made in lab with 1 M calcium chloride, 1 M HEPES, and deionized water, was added to a 50 mL beaker. A copper rod, sterilized with 70% ethanol, was placed in the gelling solution and connected to a grounded wire. The syringe was placed on an automated driver and held in place with a clamp stand with a positive wire clamped to the syringe needle. The beaker with the gelling solution was placed under the needle tip, ensuring that the needle tip was 7 mm above the meniscus of the solution. The positive wire was carefully moved until the needle tip was perpendicular to the gelling solution surface and the positive wire head not touching the beaker. The voltage on the electrostatic high voltage generator was turned on to 6 kV and the driver started. Once all polymer was expelled from the syringe, the voltage was turned off and

the syringe was quickly removed as to not create deformed microcapsules. The capsules were allowed to sink to the bottom of the beaker for 10 minutes. Once settled, the gelling solution was aspirated off and capsules were transferred into a 15 mL conical tube with cell capsule wash solution (0.15 M calcium chloride, 1 M HEPES, and deionized waer) and swirled in the washing solution for 10 seconds before being transferred to the centrifuge. Cell capsules were centrifuged at 500 RPM for 4 minutes. The cell capsule wash was removed, and the capsules were placed in a 60 mm dish with phenol-red-free DMEM and 10% FBS Ampho B media and incubated at 37^{o}C until injection. It is to be noted that all capsules that were used for experimentation did not incubate for more than 24 hours before encapsulation. To check for microcapsule consistency and fluorescence, about 500 uL of capsules were placed on a coverslip, the media was carefully removed using a Kim wipe without disturbing the capsules, and mounted using prolong diamond antifade mountant (Thermo Fisher Scientific Eugene, OR) and imaged on the Leica Stellaris 5 confocal.

Live/Dead Assay

Live/Dead assay is a fluorescent staining kit that is performed after cell encapsulation in alginate to assay cell viability and toxicity of alginate which is based on plasma membrane integrity and esterase activity. The Live/Dead Viability/Cytotoxicity kit was purchased (catalog number L3224) and performed in accordance to manufacturer protocols [64].

Injections

ARPE and ADSC microcapsules were injected into the vitreous chamber of the eye within 24 hours of microcapsule formation. The microcapsule-non phenol red media mixture was centrifuged at 500 rpm for 4 minutes, cellular media was aspirated off, and the microcapsules were transferred into a 1.5 mL microcentrifuge tube prior to injection. Mice were first anesthetized using isoflurane and eyes were dilated using 2.5% phenylephrine HCL and 1% atropine sulfate. A lubricating eye gel was then added to ensure eye hydration during injection. The sclera was then punctured at the limbus with a 26-gauge needle at a 45-degree angle with the beveled tip facing up to avoid puncturing the lens. 5 uL of microcapsules were taken and injected using a 27-gauge blunt-tip needle attached to a Hamilton syringe at a 45-degree angle. After the needle was removed, the injection site was treated with antibiotic ointments neomycin, polymyxin B sulfates, and dexamethasone ophthalmic. A 2.5% goniotaire hypromellose demulcent ophthalmic solution was applied to the eyes to prevent the cornea from drying during the recovery period. Mice were then placed on a heating pad and monitored until fully awake. Mice were kept under standardized conditions until they were sacrificed on either day 7 or day 14 post-injection.

Histology

Eyes were removed from sacrificed mice and rinsed in 1x tris-hydrochloric acid buffered saline solutuion (TBS) and immediately placed in Hartmann's Fixative (Polysciences Warrington, PA) overnight at room temperature. Hartmann's fixative, commonly known as modified Davidson's Fixative (mDF), is an alternative fixative for

ocular methods. Using mDF is important as it is safer and results in less shrinkage of the eye. Some studies have shown that mDF does not fully hold retinal morphology as in vivo [65]. As a result, 2% paraformaldehyde (PFA) was added to further hold the morphology of the retina. Samples were then washed in 1x TBS and placed in 2% PFA overnight at room temperature. Eyes were then placed in 1x TBS and sent to the Instrumentation Resource Facility at the University of South Carolina School of Medicine for paraffin embedding and sectioning. Some sections were used for hematoxylin and eosin (H&E) staining and other sections were placed in a 60°C oven for 5 minutes to melt the paraffin for immunohistochemical staining. H&E stained sections were imaged on the EVOS FL Auto Imaging System (EVOS) or the Discover Echo Revolve System (Revolve).

Immunohistochemistry Staining

Once the paraffin had melted, the sections were placed in the Leica Autostainer XL on the deparaffinization program, which sends the sections through a series of xylene, ethanol, and deionized water washes. Once removed from the autostainer, excess water was removed using a Kimwipe and the slides were allowed to air dry for 2 minutes. A PAP pen was used to draw a circle around the sections and allowed 2 minutes to dry before adding a second coat. Once the PAP pen dried, the tissue was permeabilized with 1x PBS/ 0.01M glycine/ 0.01% Triton-X 3 times for 30 minutes. The sample was then blocked in 5% goat serum for 30 minutes. Primary antibody rhodopsin or calretinin at a dilution of 1:100 was placed on the sample and placed in 4°C overnight. The next day the sample was rinsed with 1% BSA/PBS for 15 minutes two times. The sample was blocked in 5% goat serum for an hour. An Alexa Fluor 546 goat-anti-mouse secondary

antibody, as to not combat with the green CMFDA cell tracker green fluorescent cell microcapsules, at a dilution of 1:200 was used for an hour and the sample was placed in a dark location immediately after adding the secondary antibody. The sample went through a series of two washes: 1% BSA/PBS twice for 15 minutes and 1X PBS for 15 minutes. DAPI was placed on the sample at a dilution of 1:5000 for 20 minutes. The sample was quickly rinsed with 1x PBS and mounted with DABCO. Sections were imaged on the Leica Stellaris 5 confocal imaging system.

CHAPTER 3

RESULTS

Figure 3.2 represents the timeline of experimentation with 3 important time points: D0, D7, and D14. D0 is the date of injections where D7 is 1-week post-injection and D14 is 2-weeks post-injection. All eyes, whether injected or non-injected, followed this timeline.

The Live/Dead assays performed on encapsulated ARPE and ADSC cells showed that the cells are still viable once they are encapsulated as shown in Figure 3.3. This assay is dependent on plasma membrane integrity. Cells are simultaneously stained with a green and red fluorescent dyes to represent live or dead cells. The green fluorescent dye expresses intracellular esterase activity, indicative of a live cell, whereas the red fluorescent dye permeates through the plasma membrane, showing a loss of plasma membrane integrity thus representing a dead cell. This is done after sodium alginate encapsulation to ensure that sodium alginate is not affecting cell viability. It is to be noted that cell-based microcapsules stained with a live/dead assay are not the capsules that are used for eye injections. This assay has shown that 90% of cells are viable post encapsulation, representing that sodium alginate does not affect cell viability.

Figure 3.4 represents the first control group of this experiment. CMFDA-stained cell capsules are shown in Figure 3.4 A-C. These capsule images are used to compare to injected capsules to observe cell movement, cell viability, and cell release as

microcapsules open within the eye. Likewise, Figures 3.4 D-F represent a wild-type mouse eye with no injections including an H&E stain and two IHC stains for rhodopsin and calretinin. All stained images will follow this parameter of H&E stain followed by IHC rhodopsin and calretinin stains. Figure 3.3 G is a no primary control stain to ensure there is no autofluorescence within the RPE or photoreceptor layer. These images were used to compare changes within the eye of injected wildtype and knockout mice as well as retinal progression changes of non-injected knockout mice.

Figure 3.5 represents the second control group of this experiment. Figures 3.5 A-E are blank sodium alginate capsules, which means that these microcapsules do not contain any cells within them. There seems to be no effect on the cells within the eye, suggesting that sodium alginate has no adverse effect on in vivo cells. Figures 3.5 G-K are sham injections, where the injection needle punctured the eye and was removed without injecting any vehicle into the eye. These images represent that the injection method does cause unpropitious conditions within the eye like retinal detachment. The images within Figure 3.5 further prove that the materials and methodology used are a viable source for ocular injections into the vitreous chamber.

Figure 3.6 is representative of wildtype mouse eyes that were injected with ARPE microcapsules at a mouse age of 31 days and sacrificed at a mouse age of 38 days, or on D7 as according to Figure 3.2. The CMFDA-cell tracker green-labeled cells can be seen in both the rhodopsin and calretinin-stained IHC images. This is further shown in the H&E images, with the microcapsules placed within the vitreous cavity, between the ganglion cell layer and the lens. Figure 3.6 G seems to show an extra ganglion-cell layer. This is represented through the secondary line of cells that is growing next to the

microcapsule as well as the direction of the nerve fiber layers. As seen in the control eyes, the nerve fiber layer is set perpendicularly to the ganglion cell layer; however, in this newly grown ganglion cell layer, the nerve fibers are growing parallel, representing that this is a new layer of cells. A lower magnification image of this is shown in Figure 3.6 I, where multiple capsules can be seen in the vitreous cavity as well as a new nerve fiber layer and new cells within that layer. This suggests the possibility that these microcapsules produce a proximal effect within the system.

Figure 3.7 shows ARPE injected wildtype eyes at a mouse age of 31 days and sacrificed on D14. Although there seem to be no major changes in the rhodopsin staining, there is seemingly an increase in the calretinin staining. This is represented by an increase in positive staining within the ganglion cell layer as well as the nerve fiber layer. This further suggests the ideology of these cell-based microcapsules having a proximal effect within the eye.

Figure 8 shows the injection of ARPE and ADSC microcapsules into wildtype mice that were 2 and a half weeks old. This age is important because it is close to the age of symptom onset for Retinitis Pigmentosa mouse models, specifically the *Pde6b*^{rd10}/J model. ARPE-injected eyes were taken and imaged from timepoint D7 (Figure 3.8 A-E) and ADSC-injected eyes were taken and imaged from timepoints D7 (Figure 3.8 G-K) and D14 (Figure 3.8 L-P). There seem to be no major changes to these eyes except for ADSC D14 injected eyes, which seem to have a decrease in both rhodopsin and calretinin staining. These images were taken to ultimately compare to future studies of knockout mouse models at this mouse age.

Figure 8 represents adult knockout Retinitis Pigmentosa mouse eyes that were injected with ARPE capsules at D7 (Figure 3.9 A-C) and D14 (Figure 3.9 D-F) as well as a non-injected control eye at D7 (Figure 3.9 H and I) and D14 (Figure 3.9 J and K). At this age in mice, the photoreceptor layer is degraded, which can be seen in the two-nuclei layered retina instead of the three-nuclei layered retina seen in Figure 4 as well as the decreased rhodopsin and calretinin IHC staining. It can be seen that there is inflammation in these D7-injected eye within the RPE layer, which is where phagocytic activity occurs. This could be because the APRE cells seem to be attaching themselves to the lens, resulting in a decrease in vision acuity and an increase in phagocytic activity. This lens effect can also be seen in these D14-injected eyes, with the ARPE cells affecting the lens and creating slight inflammation; however, the inflammation in these D14-injected eyes is within the vitreous humor, which also contains phagocytic activity. This could represent the system reaching homeostatic stability through the phagocytic activity of the RPE and vitreous humor after these retinal cells attach to the lens, to attempt to maintain visual acuity. It can also be seen in these D14-injected eyes that there is a small portion of positive calretinin staining, which could indicate a rejuvenation of the ganglion cell layer; however, this is also seen in these D14-non-injected eyes, suggesting that it is most likely the part of the retina that was still receiving a signal from light, indicative of the 'tunnel vision' that happens within Retinitis Pigmentosa mouse models. These results suggest that ARPE cells still have a proximal effect, even if the retina is degraded.

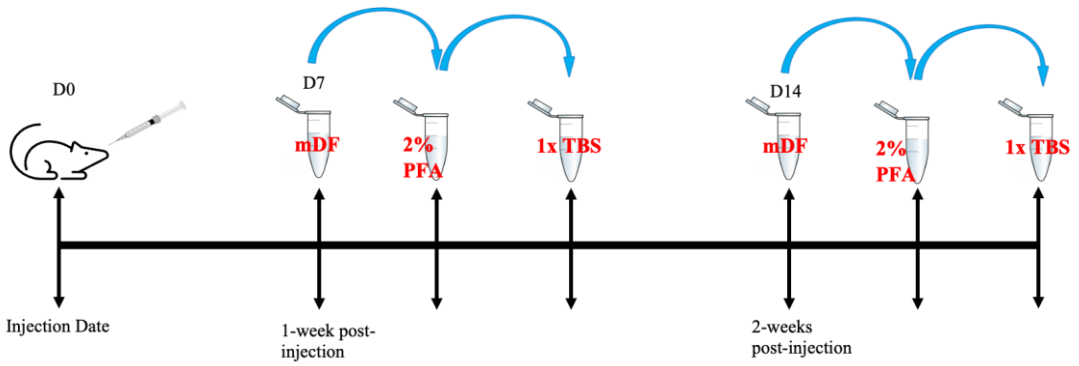

Figure 3.2: A representative timeline for days of injection: Injection date, 1-week post injection, and 2-weeks post injection known as D0, D7, and D14 respectively as well as progression of fixation.

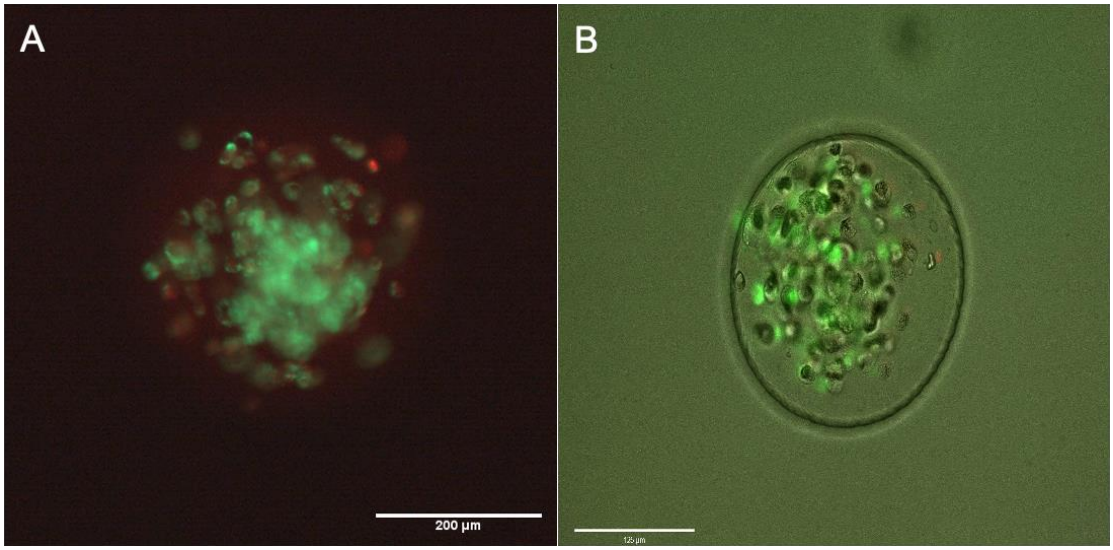

Figure 3.3: Live/Dead assay on (A) ADSC and (B) ARPE cells microcapsules.

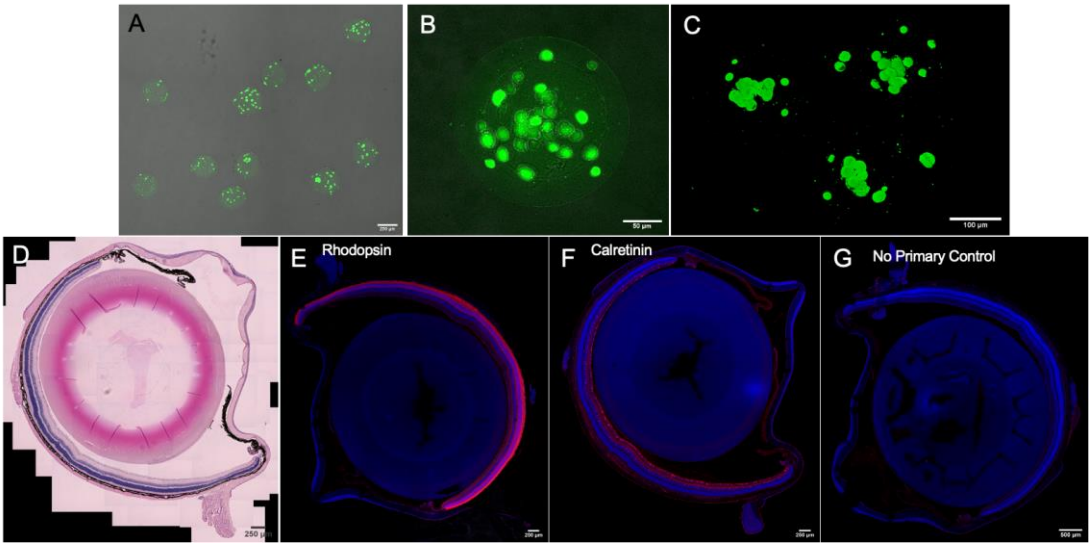

Figure 3.4: CMFDA cell tracker green stained ARPE cells in sodium alginate capsules and WT control H&E and IHC eyes. (A) Shows cell-based microcapsules at 10x magnification, (B) at 20x magnification, and (C) is a z-stack at 20x magnification. (D) is H&E 20x tile, (E) rhodopsin (F) calretinin and (G) No primary control stained 10x tiles.

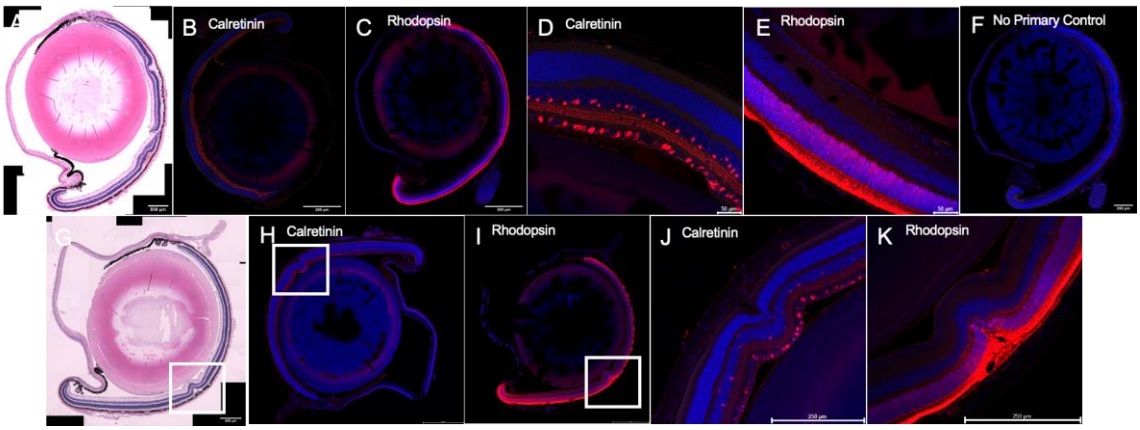

Figure 3.5: Sodium alginate microcapsules (A,B,C,D,E) in D7 mice and Sham injections (G,H,I,J,K) from D14. (A,G) H&E 20x tiled images, (B, H) calretinin 25x water tile image, (C, I) rhodopsin 25x tile images. 63x oil immersion (D) calretinin and (E). 25x water immersion (J)calretinin and (K) rhodopsin.

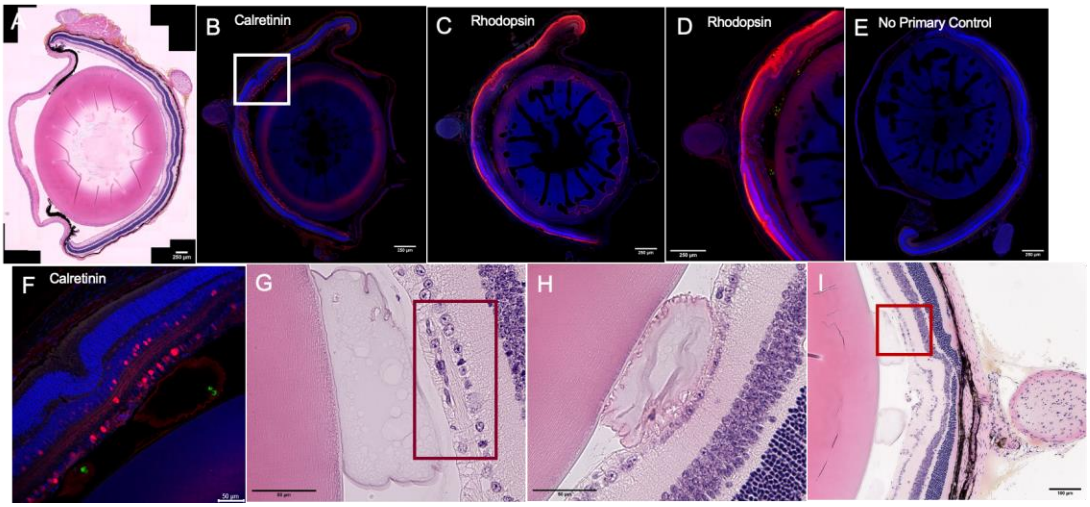

Figure 3.6: ARPE cell microcapsule injected D7 eyes of WT 4 week old mice. (A) H&E 20x tile, (B) calretinin (C) rhodopsin (E) no primary control 25x water immersion tiles. (D) rhodopsin 25x water immersion z-stack. (F) calretinin 63x oil immersion. (G) and (H) 40x H&E and (I) 10x H&E stain

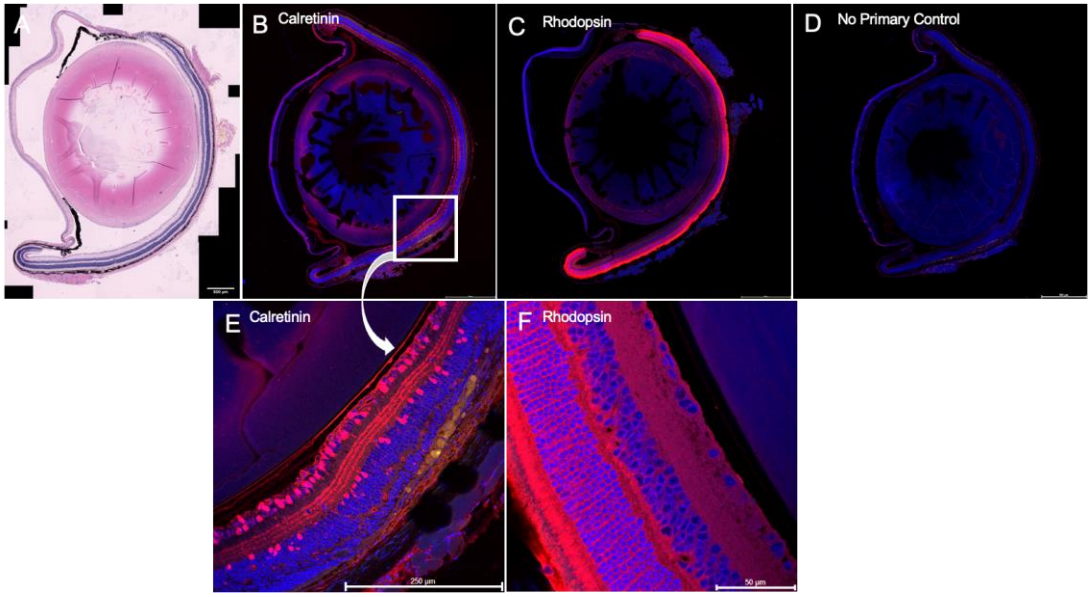

Figure 3.7: ARPE cell microcapsule injected D14 eyes of WT 4-week-old mice. (A) H&E 20x tile, (B) calretinin (C) rhodopsin (D) no primary control 25x water immersion tiles. (E) rhodopsin 63x oil immersion and (F) calretinin 63x oil immersion.

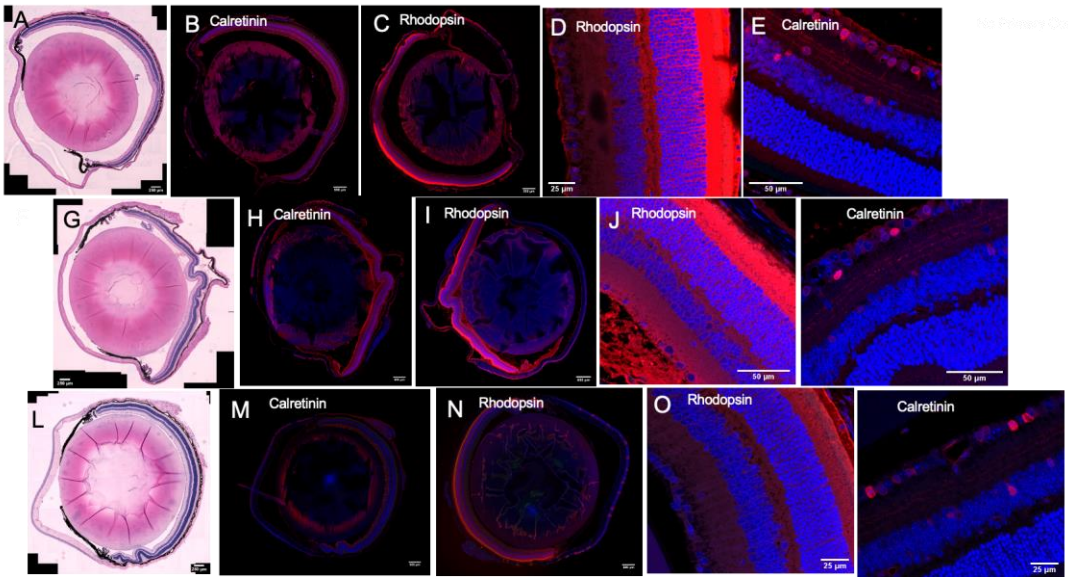

Figure 3.8: ARPE cell microcapsule injected D7 eyes and ADSC cell microcapsule injected D7 and D14 eyes of WT around 18 day old mice. (A,B,C,D,E) Represent ARPE D7 injected eyes, (F,G,H,I,J) represent ADSC D7 injected eyes, and (K,L,M,N,O) show ADSC D14 injected eyes. (A,F,K) H&E 20x tiles, (B,G,L) 10x calretinin tiles, (C,H,M) 10x rhodopsin tiles, (D,I,N) 63x oil immersion rhodopsin images, and (E,J,O) 63x oil immersion calretinin

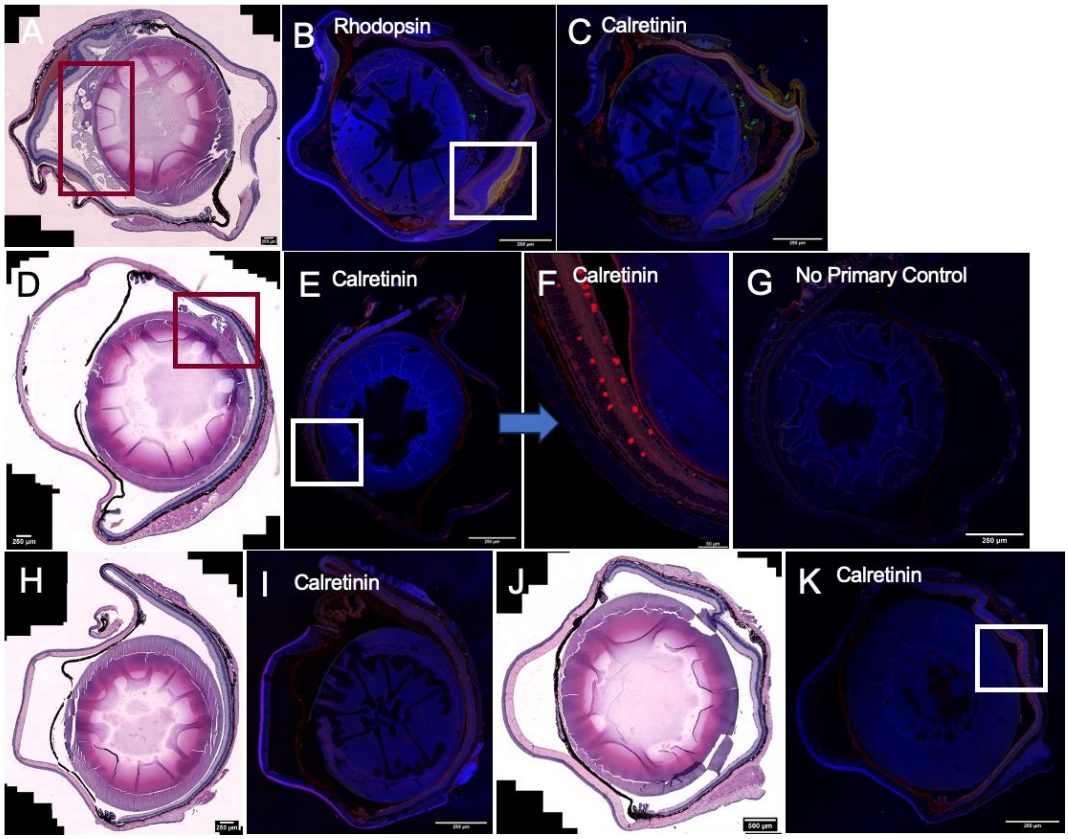

Figure 3.9: ARPE microcapsules injected and control D7 and D14 eyes in adult KO mice. (A,B,C) are ARPE injected D7 eyes, (D,E,F,) ARPE injected D14 eyes, (H,I) control D7 eyes, (J,K) control D14 eyes. (A,D,H,J) H&E 20x tiled images, (B) rhodopsin 20x tile image, (C,E,I,K) calretinin 20x tile images, (F) 63x oil immersion image, and (G) no primary control 20x tile image.

CHAPTER 4

DISCUSSION

This project suggests that cell-based sodium alginate capsules have a proximal effect within the retina, meaning that the cells are affecting either the ganglion cell layer or the retina. Figure 6 represents the ganglion cell layer being affected whereas Figure 9 represents the lens being affected. In Figure 6, there is another cellular layer growing on top of the original ganglion cell layer. This can be seen through the additional nuclei, as well as the directionality of the nerve fiber layer. This nerve fiber layer is usually perpendicular to the ganglion cell layer, where it is shown to be parallel to the new cellular growth, further showing that this is an additional layer to the retina. This can further be seen in Figure 7, where there seems to be an increase in positive calretinin staining two weeks post-injection. This suggests that ARPE cells are growing the ganglion cell layer, which could increase visual acuity.

Figure 9 shows ARPE cells affecting the lens in the knockout mice. There is a layer of cells that can be seen attached to the lens where cells should not be growing. Since the lens is created peripherally, the nuclei will form at the equator of the lens and stack on top of each other to create the crystalline structure, and these extra cells are attached to the side of the lens that is closest to the retina. At this age of mice, there should not be any nuclei found around the lens other than at the equator. This is only found in the adult knockout injected mice, which is most likely because the retinal cells

are degraded and the live injected retinal cells are attached to the working system of the lens, further proving the proximal effect of injected cell-based sodium alginate microcapsules.

Most of the D7-injected eyes have capsule visibility whereas no D14-injected eyes show capsules within them. This could show that at one point between 1 week and 2 weeks post-injection, the microcapsules are completely dispersing within the system; however, it could also represent that the 200-micron capsules are being missed within the system through histological sectioning and more research should be done within this area.

Within the IHC staining of wildtype injected eyes, there seems to be no major change in the rhodopsin-positive cells and an increase in calretinin-positive cells when using ARPE cells within the system as compared to their respective control; however, there seems to be a decrease in both rhodopsin and calretinin-positive cells when using ADSCs. This decrease in positive-stained cells while utilizing ADSCs goes against the current literature and more research should be done to further understand the effect of ADSC-based sodium alginate capsules within the eye.

This study had some limitations. The first was that some eyes were unable to be used because of either poor injection strategies that resulted in a hard, clouded eye structure from a potentially punctured lens, or poor histological sectioning where the lens or microcapsule was lost trying to achieve a specific area within the eye. These reasons are why there is not a counterpart eye for the wildtype 2-and-a-half-week-old ARPE D7 injected mice.

Another limitation is the age of the mice. For the 2-and-a-half-week-old mice, these mice are considered around 18 days old as it has not been confirmed the exact age of mice, which disrupts the concept of age-matching mice for experimental purposes. This leads to the limitation of the age of the knockout mice. The knockout mice are adult mice, meaning that their photoreceptor layer is fully degenerated, and rejuvenating the retina would be difficult at this point. For future studies, Retinitis pigmentosa knockout mice should be bread in-house as to receive young mice who can be injected at a younger age to better provide results of regenerating photoreceptor cells within the Retinitis Pigmentosa mouse models.

A final limitation is the animal-to-human reproducibility of this project. There are many differences between an animal model and a human who has any ocular disease, with the main difference being the size of the eye. As claimed in the introduction, mice have fewer cone classes and proportionally more rod photoreceptor cells as compared to humans mainly from the fact that mice are nocturnal animals. Another example is the size of the lens of mice eyes in comparison to human eyes. The lens of a mouse eye fills most of the volume within the eye resulting in a vitreous cavity that can hold around 5 uL, whereas a human lens is smaller in comparison and the vitreous cavity can hold about 3 mL [68]. With this in mind, the vitreous cavity of a human eye is about 600 times larger than a mouse eye.

Conclusion

Cell-based sodium alginate microcapsules are effective drug delivery systems for ocular diseases. This study proves that alginate is not harmful to in vitro or in vivo cells

and even shows that cells will continue to grow after the alginate capsules dissolve. Furthermore, ARPE microcapsules had a neighboring effect on either the ganglion cell layer or the lens. Wildtype mice were used from ages 18 to 45 to fully scope the effects of sodium alginate cell microcapsules on the retina through different stages of retinal development, and we have suggested that visual acuity is increased. The ability to track cell proliferation in the eye through CMFDA cell-tracker green fluorescence was crucial in fully understanding how these different cell types might affect the eye. Most of this study was done with WT mice so that future research can focus on and understand the use and effects of sodium alginate cell-based microcapsule injection as a drug delivery system for ocular diseases.

REFERENCES

1. Zhou, R. and R.R. Caspi, *Ocular immune privilege.* F1000 Biol Rep, 2010. **2**.
2. Pradeep, T., D. Mehra, and P.H. Le, *Histology, Eye*, in *StatPearls*. 2024: Treasure Island (FL).
3. Rehman, I., B. Hazhirkarzar, and B.C. Patel, *Anatomy, Head and Neck, Eye*, in *StatPearls*. 2024: Treasure Island (FL).
4. Polse, K.A., et al., *Hypoxic effects on corneal morphology and function.* Invest Ophthalmol Vis Sci, 1990. **31**(8): p. 1542-54.
5. Van Buskirk, E.M., *The anatomy of the limbus.* Eye (Lond), 1989. **3 (Pt 2)**: p. 101-8.
6. Hejtmancik, J.F. and A. Shiels, *Overview of the Lens.* Prog Mol Biol Transl Sci, 2015. **134**: p. 119-27.
7. Goel, M., et al., *Aqueous humor dynamics: a review.* Open Ophthalmol J, 2010. **4**: p. 52-9.
8. Mahabadi, N. and Y. Al Khalili, *Neuroanatomy, Retina*, in *StatPearls*. 2024: Treasure Island (FL).
9. Yang, S., J. Zhou, and D. Li, *Functions and Diseases of the Retinal Pigment Epithelium.* Front Pharmacol, 2021. **12**: p. 727870.
10. Kwon, W. and S.A. Freeman, *Phagocytosis by the Retinal Pigment Epithelium: Recognition, Resolution, Recycling.* Front Immunol, 2020. **11**: p. 604205.
11. Wang, Y., et al., *Enhanced apoptosis in retinal pigment epithelium under inflammatory stimuli and oxidative stress.* Apoptosis, 2012. **17**(11): p. 1144-55.
12. Peters, S. and U. Schraermeyer, *[Characteristics and functions of melanin in retinal pigment epithelium].* Ophthalmologe, 2001. **98**(12): p. 1181-5.
13. Mustafi, D., A.H. Engel, and K. Palczewski, *Structure of cone photoreceptors.* Prog Retin Eye Res, 2009. **28**(4): p. 289-302.
14. Hoon, M., et al., *Functional architecture of the retina: development and disease.* Prog Retin Eye Res, 2014. **42**: p. 44-84.
15. Roorda, A., et al., *Packing arrangement of the three cone classes in primate retina.* Vision Res, 2001. **41**(10-11): p. 1291-306.
16. Euler, T., et al., *Retinal bipolar cells: elementary building blocks of vision.* Nat Rev Neurosci, 2014. **15**(8): p. 507-19.
17. Grimes, W.N., *Amacrine cell-mediated input to bipolar cells: variations on a common mechanistic theme.* Vis Neurosci, 2012. **29**(1): p. 41-9.
18. Dowling, J.E., *Retina: An Overview*, in *Encyclopedia of Neuroscience*, L.R. Squire, Editor. 2009, Academic Press. p. 159-169.
19. Iuvone, P.M., *Neurotransmitters and Receptors: Dopamine*, in *Encyclopedia of the Eye*, D.A. Dartt, Editor. 2012, Academic Press. p. 130-135.

20. Rehman, I., et al., *Anatomy, Head and Neck, Eye Fovea*, in *StatPearls*. 2023: Treasure Island (FL).
21. Purves, D., et al., *The Retina*, in *Neuroscience. 2nd edition.* 2001, Sinauer Associates: Sunderland (MA).
22. Chapot, C.A., T. Euler, and T. Schubert, *How do horizontal cells 'talk' to cone photoreceptors? Different levels of complexity at the cone-horizontal cell synapse.* J Physiol, 2017. **595**(16): p. 5495-5506.
23. Jackman, S.L., et al., *A positive feedback synapse from retinal horizontal cells to cone photoreceptors.* PLoS Biol, 2011. **9**(5): p. e1001057.
24. Grassmeyer, J.J. and W.B. Thoreson, *Synaptic Ribbon Active Zones in Cone Photoreceptors Operate Independently from One Another.* Front Cell Neurosci, 2017. **11**: p. 198.
25. Kobat, S.G. and B. Turgut, *Importance of Muller Cells.* Beyoglu Eye J, 2020. **5**(2): p. 59-63.
26. Reichenbach, A. and A. Bringmann, *Glia of the human retina.* Glia, 2020. **68**(4): p. 768-796.
27. Reichenbach, A. and A. Bringmann, *New functions of Muller cells.* Glia, 2013. **61**(5): p. 651-78.
28. Marchesi, N., et al., *Ocular Neurodegenerative Diseases: Interconnection between Retina and Cortical Areas.* Cells, 2021. **10**(9).
29. Snyder, P.J., et al., *Retinal imaging in Alzheimer's and neurodegenerative diseases.* Alzheimers Dement, 2021. **17**(1): p. 103-111.
30. Ayoub, T. and N. Patel, *Age-related macular degeneration.* J R Soc Med, 2009. **102**(2): p. 56-61.
31. Tan, W., et al., *The Role of Inflammation in Age-Related Macular Degeneration.* Int J Biol Sci, 2020. **16**(15): p. 2989-3001.
32. Shu, D.Y., et al., *Role of Oxidative Stress in Ocular Diseases: A Balancing Act.* Metabolites, 2023. **13**(2).
33. O'Neal, T.B. and E.E. Luther, *Retinitis Pigmentosa*, in *StatPearls*. 2023: Treasure Island (FL).
34. Campochiaro, P.A. and T.A. Mir, *The mechanism of cone cell death in Retinitis Pigmentosa.* Prog Retin Eye Res, 2018. **62**: p. 24-37.
35. Punzo, C., K. Kornacker, and C.L. Cepko, *Stimulation of the insulin/mTOR pathway delays cone death in a mouse model of retinitis pigmentosa.* Nat Neurosci, 2009. **12**(1): p. 44-52.
36. Gopalakrishnan, P., et al., *Morphological and Functional Comparison of Mice Models for Retinitis Pigmentosa.* Adv Exp Med Biol, 2023. **1415**: p. 365-370.
37. Falsini, B., et al., *USH2A-Related Retinitis Pigmentosa: Staging of Disease Severity and Morpho-Functional Studies.* Diagnostics (Basel), 2021. **11**(2).
38. Liu, W., et al., *Retinitis Pigmentosa: Progress in Molecular Pathology and Biotherapeutical Strategies.* Int J Mol Sci, 2022. **23**(9).
39. Muradov, K.G., A.E. Granovsky, and N.O. Artemyev, *Mutation in rod PDE6 linked to congenital stationary night blindness impairs the enzyme inhibition by its gamma-subunit.* Biochemistry, 2003. **42**(11): p. 3305-10.
40. Ferrari, S., et al., *Retinitis pigmentosa: genes and disease mechanisms.* Curr Genomics, 2011. **12**(4): p. 238-49.

41. Li, B., et al., *Sex-related differences in the progressive retinal degeneration of the rd10 mouse.* Exp Eye Res, 2019. **187**: p. 107773.
42. Athanasiou, D., et al., *The molecular and cellular basis of rhodopsin retinitis pigmentosa reveals potential strategies for therapy.* Prog Retin Eye Res, 2018. **62**: p. 1-23.
43. Park, P.S., *Constitutively active rhodopsin and retinal disease.* Adv Pharmacol, 2014. **70**: p. 1-36.
44. Pahlberg, J. and A.P. Sampath, *Visual threshold is set by linear and nonlinear mechanisms in the retina that mitigate noise: how neural circuits in the retina improve the signal-to-noise ratio of the single-photon response.* Bioessays, 2011. **33**(6): p. 438-47.
45. Lee, E.S., et al., *Identification of calretinin-expressing retinal ganglion cells projecting to the mouse superior colliculus.* Cell Tissue Res, 2019. **376**(2): p. 153-163.
46. De Jong, W.H. and P.J. Borm, *Drug delivery and nanoparticles:applications and hazards.* Int J Nanomedicine, 2008. **3**(2): p. 133-49.
47. Frent, O.D., et al., *Sodium Alginate-Natural Microencapsulation Material of Polymeric Microparticles.* Int J Mol Sci, 2022. **23**(20).
48. Lengyel, M., et al., *Microparticles, Microspheres, and Microcapsules for Advanced Drug Delivery.* Scientia Pharmaceutica, 2019. **87**(3).
49. Belhaj, M., *Enhancements in Alginate Microencapsulation Technology & Impacts on Cell Therapy Development.* 2018.
50. Moore, K., et al., *Characterization of polymeric microcapsules containing a low molecular weight peptide for controlled release.* Microsc Microanal, 2013. **19**(1): p. 213-26.
51. Paredes Juarez, G.A., et al., *Immunological and technical considerations in application of alginate-based microencapsulation systems.* Front Bioeng Biotechnol, 2014. **2**: p. 26.
52. Steipel, R.T., et al., *Electrospray for generation of drug delivery and vaccine particles applied in vitro and in vivo.* Mater Sci Eng C Mater Biol Appl, 2019. **105**: p. 110070.
53. Aguilar-Toala, J.E., et al., *Encapsulation of bioactive peptides: a strategy to improve the stability, protect the nutraceutical bioactivity and support their food applications.* RSC Adv, 2022. **12**(11): p. 6449-6458.
54. Zhang, M. and X. Zhao, *Alginate hydrogel dressings for advanced wound management.* Int J Biol Macromol, 2020. **162**: p. 1414-1428.
55. Liew, C.V., et al., *Evaluation of sodium alginate as drug release modifier in matrix tablets.* Int J Pharm, 2006. **309**(1-2): p. 25-37.
56. Zhang, H., J. Cheng, and Q. Ao, *Preparation of Alginate-Based Biomaterials and Their Applications in Biomedicine.* Mar Drugs, 2021. **19**(5).
57. Mazini, L., et al., *Hopes and Limits of Adipose-Derived Stem Cells (ADSCs) and Mesenchymal Stem Cells (MSCs) in Wound Healing.* Int J Mol Sci, 2020. **21**(4).
58. Zhang, J., et al., *Adipose-Derived Stem Cells: Current Applications and Future Directions in the Regeneration of Multiple Tissues.* Stem Cells Int, 2020. **2020**: p. 8810813.

59. Piovesana, R., et al., *M2 receptors activation modulates cell growth, migration and differentiation of rat Schwann-like adipose-derived stem cells.* Cell Death Discov, 2019. **5**: p. 92.
60. Oliveira, C.R., et al., *Human Stem Cell-Derived Retinal Pigment Epithelial Cells as a Model for Drug Screening and Pre-Clinical Assays Compared to ARPE-19 Cell Line.* Int J Stem Cells, 2021. **14**(1): p. 74-84.
61. Dunn, K.C., et al., *ARPE-19, a human retinal pigment epithelial cell line with differentiated properties.* Exp Eye Res, 1996. **62**(2): p. 155-69.
62. Annamalai, B., et al., *Encapsulated Cell Technology-Based Delivery of a Complement Inhibitor Reduces Choroidal Neovascularization in a Mouse Model.* Transl Vis Sci Technol, 2018. **7**(2): p. 3.
63. McLaren, M.J., et al., *Spontaneously arising immortal cell line of rat retinal pigmented epithelial cells.* Exp Cell Res, 1993. **204**(2): p. 311-20.
64. *Thermo Fisher Scientific. (2005). LIVE/DEAD Viability/Cytotoxicity Kit for mammalian cells: User Manual. Retrieved from https://www.thermofisher.com/document-connect/document-connect.html?url=https://assets.thermofisher.com/TFS-Assets%2FLSG%2Fmanuals%2Fmp03224.pdf.*
65. Tokuda, K., et al., *Optimization of fixative solution for retinal morphology: a comparison with Davidson's fixative and other fixation solutions.* Jpn J Ophthalmol, 2018. **62**(4): p. 481-490.
66. Kono, H. and K.L. Rock, *How dying cells alert the immune system to danger.* Nat Rev Immunol, 2008. **8**(4): p. 279-89.
67. Lee, Y. and M. Overholtzer, *After-Death Functions of Cell Death.* Yale J Biol Med, 2019. **92**(4): p. 687-694.
68. Jones, G.R., *Postmortem Specimens*, in *Encyclopedia of Forensic Sciences*, P.J.S. Jay A. Siegel, Max M. Houck, Editor. 2013, Academic Press. p. 270-274.